



## Mechanical potential of eco-OSB produced from durable and nondurable species and natural resins

Olivier Arnould, Reinhard Stürzenbecher, Sandrine Bardet, Karin Hofstetter, Daniel Guibal, Nadine Amusant, Antonio Pizzi

### ► To cite this version:

Olivier Arnould, Reinhard Stürzenbecher, Sandrine Bardet, Karin Hofstetter, Daniel Guibal, et al.. Mechanical potential of eco-OSB produced from durable and nondurable species and natural resins. *Holzforschung*, De Gruyter, 2010, 64, pp.791-798. <hal-00689006>

**HAL Id: hal-00689006**

**<https://hal.archives-ouvertes.fr/hal-00689006>**

Submitted on 19 Apr 2012

**HAL** is a multi-disciplinary open access archive for the deposit and dissemination of scientific research documents, whether they are published or not. The documents may come from teaching and research institutions in France or abroad, or from public or private research centers.

L'archive ouverte pluridisciplinaire **HAL**, est destinée au dépôt et à la diffusion de documents scientifiques de niveau recherche, publiés ou non, émanant des établissements d'enseignement et de recherche français ou étrangers, des laboratoires publics ou privés.

1 Running title: **Mechanical potential of eco-OSB**  
2 **Mechanical potential of eco-OSB produced from durable and nondurable species and natural**  
3 **resins**

4 Olivier Arnould\*<sup>1</sup>, Reinhard Stürzenbecher<sup>2</sup>, Sandrine Bardet<sup>1</sup>, Karin Hofstetter<sup>2</sup>,  
5 Daniel Guibal<sup>3</sup>, Nadine Amusant<sup>3</sup> and Antonio Pizzi<sup>4</sup>

6  
7 <sup>1</sup>Laboratoire de Mécanique et Génie Civil, Université Montpellier 2, CNRS UMR5508, CC 048  
8 Place Eugène Bataillon, 34095 Montpellier, France

9 <sup>2</sup>Institute for Mechanics of Materials and Structures, Vienna University of Technology, Karlsplatz  
10 13/202, 1040 Vienna, Austria

11 <sup>3</sup>CIRAD-UR 40, 73 rue J.F. Breton, TA 10/16 34398, Montpellier Cedex 5, France

12 <sup>4</sup>Laboratoire d'Etudes et de Recherche sur le Matériau Bois, Ecole Nationale Supérieure des  
13 Technologies et Industries du Bois, Université Henri Poincaré, 27 rue du merle blanc, BP 1041,  
14 88051 Epinal Cedex 9, France

15

16 \*Corresponding Author: E-mail: olivier.arnould@univ-montp2.fr, Tel: +33 (0)4 67 14 96 50, Fax:  
17 +33 (0)4 67 14 47 92

18

19 **Abstract**

20 OSB panels were manufactured with different mixtures of pine and cypress heartwood and resins  
21 based on lignin or tannin in order to develop an eco-friendly wood composite with a natural  
22 durability against termite and fungi. Some physical properties and the major elastic moduli of bulk  
23 wood as well as of the manufactured panels were determined using different measurement  
24 techniques. In addition, a micromechanical model was adapted and validated with the experimental  
25 results. The good agreement obtained between the experimental data and model predictions  
26 indicates the proper assessment of the most influential parameters, such as raw material and  
27 adhesive properties, strand orientation, layer assembly, and density profile. A parameter study,  
28 enlightening the effect of strand orientation on several elastic constants, enlarges the scope of  
29 experiments. We conclude with an optimal combination of resin and wood species mixture resulting  
30 in the best performance from a biological and mechanical standpoint.

31

32 **Keywords:** mechanical properties, micromechanical modelling, natural resin, OSB, pine and  
33 cypress mixture

34

35 **Introduction**

36 Most of the wood-based composites are not naturally resistant to termite attack (Muin and Tsunoda  
37 2003) because they are mainly manufactured from non durable wood species. Panels designed for  
38 end uses, in which decay or termite attack are potential hazards, often contain fungicides or  
39 insecticides. Leachability and toxicity are major problems for this type of products. Nowadays, the  
40 pressure to restrict the use of wood preservatives in wood products is increasing. Moreover,  
41 interactions between adhesives and preservatives damage the bond performance and ultimately  
42 reduce the physical properties of the panel (Goroyias and Hale 2004, Kirkpatrick and Barnes 2006).  
43 Thus, alternative approaches are necessary to obtain good durability of environmentally friendly  
44 wood composites without loss of performance.

45 Modern product developments should consider both ecological and technical aspects. The  
46 resistance of wood products to biodegradation can be increased by using naturally durable wood  
47 species, especially in regions with low to moderate termite hazard (Behr 1972, Yalinkilic et al.  
48 1998, Evans et al. 2000, Kartal and Green 2003, Wan et al. 2007). Another environmental concern  
49 is the control of volatile and semi-volatile compounds derived mainly from adhesives (resins).  
50 Natural resins based on lignin (Lei et al. 2007, Mansouri et al. 2007a) or tannin (Garnier et al. 2002,  
51 Ballerini et al. 2005) are options for environment-friendly products.

52 A political concern nowadays is on reducing the emission of climate gases (mainly CO<sub>2</sub>) in  
53 production processes. Wood and wood products are a priori ecological materials, especially if  
54 productions processes are well optimized with reduced energy consumption (ECOSB 2008) and  
55 residues (by-products). Oriented strand board (OSB) panels are exemplary with this regard as their  
56 production permits the utilization of almost all the harvested trees including imperfect or young  
57 trees and fast growing species.

58 Results on the durability of ecological OSB products (shortly ‘eco-OSB’) have been  
59 published recently (Amusant et al. 2009). It has been shown that OSB made of a mixture of  
60 heartwood cypress (*Cupressus sempervirens*) and pine (*Pinus sylvestris*), with lignin (with

61 paraformaldehyde and pMDI) or tannin (from pine with hexamine hardener)-based resin, show  
62 durability against termites and fungi.

63 The load bearing capacity of OSB panels in structural applications is essential. Thus, this  
64 paper focuses on the mechanical potential of these eco-OSBs. Firstly, mechanical properties of the  
65 raw material and of eco-OSB will be identified by several mechanical testing methods. Secondly, a  
66 micromechanical model will be applied, which provides a link between microstructural  
67 characteristics and the macroscopic mechanical behaviour. In particular, the overall elastic  
68 properties of the panels will be estimated considering the physical properties of bulk wood and resin  
69 as well as the morphological characteristics of the OSB such as strand orientation, density profile  
70 and layer assembly. The motivation for the modelling is to further explore the mechanical potential  
71 of the panels beyond the traditional experiences. The micromechanical model should serve as the  
72 basis for product development and optimisation. The expectation is that it allows identifying  
73 optimal panel designs in terms of microstructural characteristics and panel lay-ups.

74

## 75 **Materials and methods**

### 76 Characterization of the raw materials

77 OSB was produced of cypress heartwood, which is naturally durable against termites, and sap- and  
78 heart-wood of pine, which are both nondurable against termites. The different 60-year old trees  
79 were grown in the Grenouillet Arboretum (France), felled, and crosscut into 1 m long logs. Test  
80 specimens for determination of physical and mechanical properties were cut from the logs as  
81 depicted in Figure 1. All specimens, i.e., the raw material and the OSB panels, were conditioned  
82 and tested at a temperature of 20°C and a relative humidity (RH) of 65%. First, static compression  
83 tests on cubes, with a side length of 40 mm machined along the principal material directions (R, T  
84 and L) were performed on a universal electromechanical testing machine MTS 1/ME with a 5 kN  
85 load cell. Mean compression strain was assessed by using strain gages (from Kyowa and TML with  
86 2 or 8 mm gage length depending on the annual ring thickness on the face considered) for

87 calculating the elastic moduli  $E_R$ ,  $E_T$  and  $E_L$ . Moreover, transversally oriented gages were used to  
 88 measure the transverse strains on each of the four accessible faces of the cubes for determination of  
 89 the six Poisson's ratios  $\nu_{RT}$ ,  $\nu_{TR}$ ,  $\nu_{LT}$ ,  $\nu_{TL}$ ,  $\nu_{LR}$  and  $\nu_{RL}$ . The maximum applied load corresponds to a  
 90 mean compressive strain of around 0.2%. The test consists in three loading/unloading cycles at a  
 91 strain rate of about  $10^{-4} \text{ s}^{-1}$ . The elastic moduli are measured in the linear range of the  
 92 unloading/reloading curves.

93 In addition, Bordonné's free vibration beam method (Bordonné 1989, Brancheriau and  
 94 Bailleres 2002) was applied on samples sized  $20 \times 20 \times 360 \text{ mm}^3$  (R-T-L). It allows measuring  
 95 longitudinal bending elastic modulus,  $E_L$ , and shear moduli,  $G_{TL}$  or  $G_{LR}$  depending on the sample  
 96 rotation along the L-direction, at the natural frequency of the beam, which is approximately 700 Hz.  
 97 Furthermore, ultrasound measurements in the directions of the principal axes have been performed  
 98 by means of Sofranel's 1 MHz longitudinal transducer on cubes with side lengths of 20 mm cut at  
 99 the end of the free vibration beam (see Figure 1). Determining the ultrasound velocity  $V$  in the  
 100 sample (Bucur 2005) and knowing the density  $\rho$ , it is possible to compute the elastic stiffness  $C_{ii}$  of  
 101 the sample that is linked to the modulus of elasticity  $E_i$  and the Poisson's ratios  $\nu_{ij}$  (Guitard 1989):

$$102 \quad E_i = \frac{1 - \nu_{TR}\nu_{RL}\nu_{LT} - \nu_{LR}\nu_{RT}\nu_{TL} - (\nu_{TL}\nu_{LT} + \nu_{TR}\nu_{RT} + \nu_{LR}\nu_{RL})}{1 - \nu_{jk}\nu_{kj}} C_{ii} \quad (1)$$

103 where  $C_{ii} = \rho V_i^2$  and  $i, j, k = \{R, T, L\}$ , e.g., if  $i = R$  then  $1 - \nu_{jk}\nu_{kj} = 1 - \nu_{TL}\nu_{LT}$ . Assuming a negligible  
 104 effect of loading frequency on the Poisson's ratios, their values obtained with the compression tests  
 105 are used to compute the elastic modulus  $E_i$  from  $C_{ii}$ .

106 A micromechanical model by Hofstetter et al. (2005, 2006, 2007) was also applied because a  
 107 complete and consistent set of all nine independent elastic constants of the bulk wood was not  
 108 always available or reliable. This model allows the prediction of the elasticity tensor of various  
 109 wood species from the elastic properties of the basic constituents of wood (cellulose,  
 110 hemicelluloses, lignin and water) and from morphological parameters such as microfibril angle  
 111 (MFA), cell arrangement and macroscopic density. In order to estimate the properties of the raw

112 material, density was chosen in accordance with the mean density of the tested bulk wood samples.  
113 The microstructural characteristics, MFA and the lignin content, were determined by adjusting the  
114 resulting model predictions of  $E_L$ ,  $E_T$  and  $G_{TL}$  to the corresponding experimental results from  
115 bending free vibration and compression tests. The model estimated stiffness tensor obtained for  
116 these microstructural characteristics was finally used as input for the panel model presented below.

#### 117 Manufacturing OSB panels

118 Flakes with dimensions of  $0.6 \times 10 \times 100 \text{ mm}^3$  (R-T-L) were manually trimmed in thin veneers and  
119 the flakes of each species were dried to about 6–7% moisture content (MC) before gluing. Mat  
120 formation and strand orientation were done by hand. The full set of panel manufacturing parameters  
121 is presented in Table 1. A total of 24 OSB panels was prepared, which corresponds to three panels  
122 for each combination of resin and species.

#### 123 Characterization of OSB test specimens

124 From each panel, 18 squared test specimens with dimensions of  $50 \times 50 \times 14 \text{ mm}^3$  and 2 beams (one  
125 sized  $300 \times 40 \times 14 \text{ mm}^3$ , mainly oriented in the  $x$ -direction, and one sized  $260 \times 40 \times 14 \text{ mm}^3$ , mainly  
126 oriented in the  $y$ -direction) were cut (Figure 2). The beams and part of the squared specimens were  
127 used for determination of the elastic properties of the panels, while the remaining squared  
128 specimens were employed for the durability measurements (Amusant et al. 2009).

129 The mean density was measured for each test specimen. The vertical density profile was  
130 determined by means of the densitometer DENSE-LABX (Electronic Wood System, Germany) at  
131 increments of 0.05 mm for ten randomly chosen specimens. The strand orientation distribution was  
132 determined manually using pictures of the outer surfaces of three different panels (Figure 2) and  
133 ImageJ, a public domain image processing software.

134 Classical static face down 4 point-bending test (outer span: 250 mm, inner span: 160 mm,  
135 loading point diameter: 20 mm) were first done on the beam-shaped sample using again the  
136 electromechanical testing machine MTS 1/ME equipped with a 5 kN load cell, at a loading speed of  
137  $10 \mu\text{m s}^{-1}$  in order to reach the ultimate loading force in  $300 \pm 120 \text{ s}$  following EN 789 European

138 standard (2005). The tests were performed in the elastic range, and the bending strain was measured  
139 through the difference in deflection between three points by means of a micrometer mounted on a  
140 specific fitting. Accordingly, the static bending moduli of elasticity in the two main panel  
141 directions,  $E_x$  and  $E_y$ , were obtained. In addition, the same samples were tested in free vibration  
142 bending using Bordonné's principle (Bordonné 1989, Brancheriau and Bailleres 2002). Face down  
143 measurements allow to determine the bending moduli of elasticity,  $E_x$  and  $E_y$ , at a frequency of  
144 around 500 Hz and edgewise measurements yield estimates of the shear elastic modulus  $G_{xy}$   
145 (Brancheriau 2006) on the two types of beams ( $x$  and  $y$ -direction). Finally, ultrasound  
146 measurements through the thickness of the squared specimens were performed in order to obtain the  
147 elastic stiffness  $C_{zz}$ .

#### 148 Modelling the elastic properties of the panels

149 A multiscale model for strand-based engineered wood products developed by Stürzenbecher et al.  
150 (2010a, b) was applied and adapted to the specific characteristics of the present panels. This  
151 multiscale model is based on the continuum micromechanics and lamination theory and predicts the  
152 in-plane tension and bending stiffnesses as well as the in-plane shear stiffness of multi-layer strand  
153 boards. Thereby, the boards are idealized consisting of ellipsoidally shaped and perfectly bonded  
154 wood strands. The following parameters are considered: the elastic properties of the wood species,  
155 the slenderness ratio and orientation distribution of the strands, as well as the panel lay-up described  
156 in terms of density profile and layer assembly. Here only the specifications of the model for the  
157 present study are explained. For a detailed description of the model approach, see Stürzenbecher et  
158 al. (2010b). The high resin mass content of the produced boards (Table 1), which equals about 6%  
159 (by volume) of the final boards, requires an adjustment of the original model. This model had been  
160 developed for strand boards with moderately low resin content, which did not necessitate  
161 consideration of the adhesive as a separate material phase. In order to account properly for the  
162 higher adhesive content in this application, strands were modelled with an adhesive layer, applying  
163 the Composite Cylinder Assemblage (CCA) model for estimating their elastic properties (Hashin

164 and Rosen 1964, Hashin 1979). The transverse shear modulus, which cannot be estimated by means  
165 of the CCA model, was predicted by a Generalised Self Consistent Scheme developed by  
166 Christensen and Lo (1979). Based on the estimated elastic properties of adhesive coated strands, the  
167 homogenization procedure of Stürzenbecher et al. (2010b) was applied, accounting for the  
168 compaction, the strand orientation distribution, the layer assembly and the density profile across the  
169 panel thickness. The elastic behaviour of the tannin and the lignin adhesives in their cured state was  
170 assumed to be isotropic with a Poisson's ratio of 0.3 and a modulus of 1.8 GPa (Garcia and Pizzi  
171 1998, Osman and Pizzi 2002) and 2.1 GPa (Mansouri et al. 2007b), respectively. Since the density  
172 profiles were not measured at every test specimen, one characteristic representative of all measured  
173 density profile was taken for modelling of all panels. This procedure was feasible, since the  
174 production process was the same for all panel types and only little variation was observed between  
175 the measured density profiles.

176 Extending the original model by Stürzenbecher et al. (2010b), the stiffness component  $C_{zz}$  in the  
177 plate thickness direction was estimated from the respective values of the individual board layers  
178 with different densities. This was done using the rule of mixtures for serially arranged materials,  
179 reading mathematically as:

$$180 \quad C_{zz} = \frac{1}{\sum_{i=1}^N \frac{f_i}{C_{zz_i}}} \quad (2)$$

181 where  $f_i$  denotes the relative layer thickness and  $C_{zz_i}$  the stiffness tensor component of this layer  $i$   
182 in the thickness direction of the panel.

183

## 184 **Results and discussion**

### 185 Density and mechanical properties of the raw materials

186 The data for density and elastic properties of the bulk wood are reported in Table 2. For the static  
187 compression tests, only one sample per species was tested several times. This may explain the very  
188 low standard deviation of the respective results. For the compression tests on pine, Poisson's ratio



189  $\nu_{LR}$  is missing because of experimental difficulties. The measurement of Poisson's ratio  $\nu_{LT}$  is  
190 difficult as well, leading to too high values on one side of the sample, of only limited reliability, that  
191 leads to the high standard deviation reported. The values for  $\nu_{LT}$  have been checked by measuring  
192  $\nu_{TL}$  as well, but the measurement results were not better in this case due to the small absolute values  
193 of these ratios. The results for the longitudinal elastic moduli,  $E_L$ , of the raw material measured by  
194 different techniques are in reasonably good agreement with each other. Similarly good agreement is  
195 obtained for the elastic moduli  $E_T$  and  $E_R$  determined by ultrasound measurements and static  
196 compression tests. The beam free vibration measurements delivered in addition to the  $E_L$  both shear  
197 moduli  $G_{TL}$  and  $G_{LR}$ . Values obtained with this last method for  $E_L$  are in good agreement with the  
198 other ones even if it corresponds in that case to bending loading. This may be due to the relatively  
199 good homogeneity of the material at the considered cross section scale.

200         Microstructural characteristics of bulk wood were back-calculated by the micromechanical  
201 model (Hofstetter et al. 2005, 2006, 2007) based on the values of  $E_L$ ,  $E_T$  and  $G_{TL}$  measured with the  
202 bending free vibration technique. MFAs of  $21^\circ$  were obtained for pine and  $22^\circ$  for cypress, whereby  
203 the lignin content of the former was 20% and 26% of the latter, which is in the range of possible  
204 mean lignin contents for softwood from 25 to 34% after Petterson (1984) or from 20% to 27% after  
205 Faix (2008). Accordingly, the micromechanical model provides a full set of elastic constants of the  
206 (orthotropic) raw material, which is in full agreement with those obtained from experiments  
207 (Table 2).

#### 208 Structural characterization of the produced strand boards

209 The average density of all panels is about  $656 \text{ kg m}^{-3}$  with a standard deviation of  $24 \text{ kg m}^{-3}$ . Figure  
210 3 shows the characteristic measured density profile, which was used for the evaluation of the model  
211 for eco-OSB panels. It exhibits a moderate U-shape, as all the measured density profiles. For  
212 modelling purpose, this profile was discretized: constant density values were determined for layer  
213 thicknesses between 0.5 mm close to the surfaces and 2.5 mm in the centre of the board (Figure 3).

214 The strand orientation distribution measured on the surfaces of three different panels is depicted in  
215 Figure 4. A classical spread of orientations is observed, and a normal distribution was adjusted by  
216 the least-square method. This yields a mean orientation close to  $0^\circ$  and a standard deviation around  
217  $5^\circ$ , reflecting the careful panel production by hand, which achieves better alignment of strands than  
218 industrial processes.

#### 219 Mechanical properties of the produced strand boards

220 The elastic properties of the final OSBs, measured with different techniques, are presented in Table  
221 3 and grouped according to the mixture of wood species and the resin types. Here, the medians and  
222 the ranges are given, showing the difference between the maxima and the minima of the three  
223 replicates of each setting.

224 The values obtained in static bending are in good agreement with those obtained in free  
225 vibration despite the difference in the loading frequency. Free vibration yielded quite similar results  
226 for the in-plane shear-modulus obtained for the beams oriented in  $x$  and  $y$ -direction. The order of  
227 the values of the measured moduli is as expected, i.e.,  $E_x > E_y > G_{xy}$ , because  $E_x$  and  $E_y$  are mainly  
228 linked to  $E_L$  and  $E_T$  of the bulk wood, respectively, as the outer layers contribute dominantly to the  
229 overall bending stiffness of the panels. Remarkably, the results for the elastic moduli do not  
230 correlate with the amount of cypress in the mixture except for the stiffness  $C_{zz}$ . The latter decreases  
231 when the amount of cypress is reduced irrespective of the resin. This is in line with the slightly  
232 higher moduli  $E_R$  measured on the bulk wood samples of cypress than on those of pine. For the  
233 bending moduli  $E_x$  and  $E_y$  measured on the panel, the effect of cypress content is not obvious,  
234 probably because the two moduli of the bulk material controlling the panel bending stiffness,  
235 namely  $E_T$  and  $E_L$ , are close to each other for the two species, as can be seen in Table 2. The  
236 variability of the out-of-plane modulus rather results from variations of the wood and resin  
237 properties in individual panels than from different extents of bonding defects. On the other hand,  
238 the variability of the bending properties of the panels is – amongst others – a consequence of  
239 varying bonding quality between strands. Altogether, the mechanical properties were comparable to

240 that of conventional, industrially produced boards, highlighting the potential of the investigated bio-  
241 composite. In this study, panels made with lignin-based resin give the best results in terms of elastic  
242 properties. This is all the more interesting as lignin-based resin yields the best durability too  
243 (Amusant et al. 2009).

#### 244 Comparison of model predictions and experimental results

245 The suitability of the micromechanical model was validated experimentally. For this purpose, the  
246 model is evaluated with the specifications of the produced boards, including the elastic properties of  
247 the raw material and resin, the characteristic density profile adjusted to the mean final density, the  
248 strand orientation distribution and the layer assembly. Thereupon, a one-to-one comparison is made  
249 between the model estimates and the corresponding results of bending free vibration tests ( $E_x$ ,  $E_y$   
250 and  $G_{xy}$ ) and ultrasonic experiments ( $C_{zz}$ ), respectively (Figure 5). Both MOE,  $E_x$ , and  $E_y$ , estimated  
251 by the model show on average good agreement with the experimental results obtained from bending  
252 free vibration tests. Natural fluctuations of elastic properties of the raw material and variations in  
253 the production process were not considered in the model, so that the considerable variations of the  
254 experimental results were not reproduced by the model. The mean prediction error of the MOE  $E_x$   
255 amounts to 12.1% with a standard deviation of 17.1%, while it is 3.8% with a standard deviation of  
256 21.4% for  $E_y$ . The in-plane shear modulus  $G_{xy}$  is overestimated by the model by 24.6% with a  
257 standard deviation of prediction errors of 46.5%. Particularly, experimental shear moduli below  
258 1 GPa are not well predicted by the model. Further, the model overestimated the transverse stiffness  
259 component  $C_{zz}$  by about 24.6%, with a standard deviation of 35.2%.

#### 260 Model parameter studies on the effect of strand orientation

261 The experimentally validated model was extended to the experimental investigations of the  
262 mechanical behaviour of eco-OSB to non-tested configurations. Particular emphasis is placed on  
263 examining the effect of strand orientation distribution on the elastic properties of the final panels.  
264 The strand orientation of industrially produced boards is expected to be not as strictly oriented as  
265 currently observed in the hand-made panels. Taking this into consideration, the model allows

266 estimating elastic properties of panels from a commercial production line. The parameter study is  
267 performed for pine wood as raw material, lignin adhesive, and a mean board density of  $650 \text{ kg m}^{-3}$ .  
268 Adhesive content, density profile, and the ratio of strand mass in the face and core layers  
269 respectively, are the same as in the actually produced boards considered in the model validation.

270 The distribution of strand orientation is described by a normal distribution with a mean  
271 orientation of  $0^\circ$  (coinciding with the  $x$ -axis) and a variable standard deviation. Increasing the  
272 standard deviation finally leads to a random strand orientation distribution. Figure 6 shows the  
273 pronounced effect of less tight strand orientation, modelled by increasing the standard deviation of  
274 the assumed normal distribution, on the mechanical properties of the panel. The MOE in the  
275 principal direction of the panel decreases dramatically when the strands are less aligned with the  
276 principal panel direction, whereas the MOE perpendicular to this direction increases only slightly.  
277 The in-plane shear modulus  $G_{xy}$  rises with increasing standard deviation of the strand orientation  
278 distribution from about 1.4 GPa to about 2.5 GPa. This means that higher deviations of strand  
279 orientations from the main panel direction in commercial production, improves the performance of  
280 the panel for shear stiffening applications, but degrades it for bending applications with a single  
281 pronounced load bearing direction.

282

## 283 **Conclusion**

284 Characterization of wood species as raw materials for OSB production with various methods (static  
285 vs. dynamic and compression vs. bending) led to very similar and satisfactory results. This good  
286 agreement is due to the low viscosity of dry wood and the relatively high homogeneity of the  
287 sample in the scales of L-direction and cross section (i.e., relatively small annual ring width  
288 compared to the cross section characteristic length). Additionally, a micromechanics model was  
289 applied delivering all stiffness components of the input wood and, thus, completing the  
290 characterization. The mechanical behaviour of the laboratory-made panels was also determined by  
291 dynamic and static measurement techniques. The best quality (with highest stiffness) has been

292 obtained for the panels glued with lignin-based resin. As this type of panels show the best durability  
293 too, they might be suitable for developing eco-OSB panels at the industrial scale. Further, a multi-  
294 scale model has been developed and applied in order to explore and to quantify the influences of the  
295 microstructural characteristics on the mechanical behaviour of the boards for non-tested  
296 configurations. The established model for eco-OSB is able to reflect suitably the microstructural  
297 characteristics of raw material and adhesive properties, strand orientation, density profile and layer  
298 assembly. It delivers reasonably accurate predictions for the mean elastic properties, e.g., both the  
299 in-plane bending moduli and the in-plane shear modulus as well as the out-of-plane or transverse  
300 stiffness tensor component. Employing the validated model for parameter studies gives insight into  
301 the (micro)mechanical behaviour of strand boards. In an exemplary manner, the effect of strand  
302 orientation distribution on bending and shear stiffness was demonstrated to be able to estimate the  
303 influence of the production process on the mechanical properties of the panels. The combination of  
304 the theoretical model, capable to describe the underlying mechanics, and complementary  
305 experiments, affording direct insight into the mechanical performance, seems to be a fruitful and  
306 efficient approach. This combination permits the further development of products.

307

### 308 **Acknowledgements**

309 The authors gratefully acknowledge Remy Marchal and Jean Claude Buteaud (from the Labomap  
310 laboratory, Ecole Nationale Supérieure d'Arts et Métiers, Cluny, France) for the peeling of the  
311 strands.

## References

- Amusant, N., Arnould, O., Pizzi, A., Depres, A., Mansouris, R.H., Bardet, S., Baudassé, C. (2009) Biological properties of an OSB eco-product manufactured from a mixture of durable and non durable species and natural resins. *Eur. J. Wood Prod.* 67:439-447
- Ballerini, A., Depres, A., Pizzi, A. (2005) Non-toxic, zero-emission tannin-glyoxal adhesives for wood panels. *Holz Roh Werkst.* 63(6):477-478
- Behr, E.A. (1972) Decay and termite resistance of medium density fiberboards made from wood residue. *For. Prod J.* 22(12):48-51
- Bordonné, P.A. (1989) Module dynamique et frottement intérieur dans le bois, mesures sur poutres flottantes en vibrations naturelles. Ph.D. thesis, Institut National Polytechnique de Lorraine.
- Brancheriau L. (2006) Influence of cross section dimensions on Timoshenko's shear factor – Application to wooden beams in free-free flexural vibration. *Ann. For. Sci.* 63:319-321
- Brancheriau, L., Bailleres, H. (2002) Natural vibration analysis of clear wooden beams: a theoretical review. *Wood Sci. Technol.* 36:347-365
- Bucur, V. Acoustics of wood. 2nd revised edition, Springer-Verlag, Berlin, 2005.
- Christensen, R.M., Lo, K.H. (1979) Solutions for effective shear properties in three phase sphere and cylinder models. *J. Mech. Phys. Solids* 27:315-330
- ECOSB Layman's report (2008) New and environmentally friendly OSB panels. LIFE Project LIFE05 ENV/L/000047
- European standard (2005) EN 789. Timber structures – Test methods – Determination of mechanical properties of wood based panels
- Evans, P.D., Dimitriade, S., Cunningham, R.B., Donnelly, C.F. (2000) Medium density fibreboard manufactured from blends of white cypress pine and non-durable wood species shows increased resistance to attack by subterranean *C. lacteus*. *Holzforschung* 54(6):585-590
- Faix, O. (2008) Chemie des Holzes. In: Taschenbuch der Holztechnik. Eds. Wagenführ, A., Scholz, F. Hanser Verlag, München. pp. 47-74
- Garcia, R., Pizzi, A. (1998) Polycondensation and autocondensation networks in polyflavonoid tannins. II. Polycondensation versus autocondensation. *J. Appl. Poly. Sci.* 70:1093-1109
- Garnier, S., Pizzi, A., Vorster, O., Halasz, L. (2002) Rheology of polyflavonoid tannin-formaldehyde reactions before and after gelling - Part 2: Hardener influence and comparison of different tannins. *J. Appl. Poly. Sci.* 84(4):864-871
- Goroyias, G.J., Hale, M.D. (2004) The mechanical and physical properties of strand boards treated with preservatives at different stages of manufacture. *Wood Sci. Technol.* 38:93-107
- Guitard, D. Mécanique du matériau bois et composites. Cépaduès, Toulouse, France, 1987
- Hashin, Z. (1979) Analysis of properties of fiber composites with anisotropic constituents. *J. Appl. Mech.* 46:543-550
- Hashin, Z., Rosen, B.W. (1964) The elastic moduli of fiber-reinforced materials. *J. Appl. Mech* 31:223-232
- Hofstetter, K., Hellmich, Ch., Eberhardsteiner, J. (2005) Development and experimental verification of a continuum micromechanics model for wood. *Eur. J. Mech. A/Solids* 24:1030-1053
- Hofstetter, K., Hellmich, Ch., Eberhardsteiner, J. (2006) The influence of the microfibril angle of wood stiffness: a continuum micromechanics approach. *Comput. Assist. Mech. Eng. Sci.* 13:523-536

- Hofstetter, K., Hellmich, Ch., Eberhardsteiner, J. (2007) Micromechanical modeling of solid-type and plate-type deformation patterns within softwood materials. A review and an improved approach. *Holzforschung* 61(4):343-351
- Kartal, S.N., Green III, F. (2003) Decay and termite resistance of medium density fibreboard (MDF) made from different wood species. *Inter. Biodeter. Biodegr.* 51:29-35
- Kirkpatrick, J.W., Barnes, H.M. (2006) Biocide treatments for wood composites – A review. In: 37th annual meeting of the International Research Group on Wood Preservation. IRG/WP 06-40323. 21 p
- Lei, H., Pizzi, A., Du, G. (2007) Environment-friendly, mixed tannin/lignin wood resins. *J. Appl. Poly. Sci.* 107(1):203-209
- Mansouri, N.E., Pizzi, A., Salvado, J. (2007a) Lignin-based wood panel adhesives without formaldehyde. *Holz Roh Werkst.* 65(1):65-70
- Mansouri, N.E., Pizzi, A., Salvado, J. (2007b) Lignin-based polycondensation resins for wood adhesives. *J. Appl. Pol. Sci.* 103:1690-1699
- Muin, M., Tsunoda, K. (2003) Termicidal performance of wood based composites treated with silafluofen using supercritical carbon dioxide. *Holzforschung* 57(6):585-592
- Osman, Z., Pizzi, A. (2002) Comparison of gelling reaction effectiveness of procyanidin tannins for wood adhesives. *Hols Roh Werkst.* 60:328
- Petterson, R.C. (1984) The chemical composition of wood. In: *The chemistry of solid wood*. Eds. Rowell, R. American Chemical Society, Washington D.C. pp. 57-126
- Stürzenbecher, R., Hofstetter, K., Bogensperger, Th., Schickhofer, G., Eberhardsteiner, J. (2010a) Development of high-performance strand boards: engineering design and experimental investigations. *Wood Sci. Technol.* 44(1):13-29
- Stürzenbecher, R., Hofstetter, K., Schickhofer, G., Eberhardsteiner, J. (2010b) Development of high-performance strand boards: multiscale modeling of anisotropic elasticity. *Wood Sci. Technol.* 44(2):205-223
- Wan, H., Wang, X.M., Yang, D.Q. (2007) Utilizing eastern white Cedar to improve the resistance of strand boards to mold and decay fungi. *For. Prod. J.* 57(3):54-59
- Yalinkilic, M.K., Imamura, Y., Takahashi, M., Kakaycioglu, H., Dermici, G.N., Ozdemir, T. (1998) Biological, physical and mechanical properties of particleboards manufactured from waste leaves. *Inter. Biodeter. Biodegr.* 41:75-84

Table 1. Parameters of panel manufacturing

Panel dimensions	350×350×14 mm <sup>3</sup>
Three layers panel construction	Core perpendicular to face flakes
Mass distribution (side/core/side)	20% / 60% / 20%
Wood species	Pine, cypress
Target mat moisture content	6-7%
Resin mass content	13% side and 11% core
Blender type for mixing strands with resin	Dakota
Blender rotation speed	900 rpm
Pressing cycle for gluing	90 s 35 bar, 120 s 16 bar, 150 s 8 bar
Press temperature	175°C (plate surface)
Total press time	6 min
Replicate	3



1 Table 2. Mean values of measured wood bulk properties obtained by different measurement methods and by micromechanical model predictions for  
 2 the nine independent elastic constants of bulk wood.

Wood	Properties	Beam free vibration (~700 Hz) Sample: 20 × 20 × 360 mm <sup>3</sup>	Ultrasound (1 MHz)	Static compression test Sample: 40 × 40 × 40 mm <sup>3</sup>	Computed
Cypress ( <i>Cupressus sempervirens</i> )	$\rho$ (kg m <sup>-3</sup> )	579±4	569±8	580	
	$E_R$ (GPa)		1.99±0.09	1.75±0.03	1.21
	$E_T$ (GPa)		1.44±0.08	1.16±0.04	0.86
	$E_L$ (GPa)	13.17±0.97	12.55±0.96	11.21±1.79	13.03
	$\nu_{RT}$			0.63±0.05	0.49
	$\nu_{LR}$			0.36±0.03	0.32
	$\nu_{LT}$			0.71±0.22	0.37
	$G_{TL}$ (GPa)	1.00±0.01			1.00
	$G_{LR}$ (GPa)	1.12±0.06			1.02
	$G_{RT}$ (GPa)				0.12
Pine ( <i>Pinus sylvestris</i> )	$\rho$ (kg m <sup>-3</sup> )	547±26	537±21	535	550
	$E_R$ (GPa)		1.86±0.12	1.79±0.01	1.13
	$E_T$ (GPa)		0.73±0.19	0.91±0.01	0.80
	$E_L$ (GPa)	14.39±1.73	13.99±1.12	15.85±0.25	13.84
	$\nu_{RT}$			0.58±0.14	0.52
	$\nu_{LR}$			--	0.32
	$\nu_{LT}$			0.61±0.29	0.36
	$G_{TL}$ (GPa)	1.02±0.09			0.98
	$G_{LR}$ (GPa)	1.37±0.10			1.00
	$G_{RT}$ (GPa)				0.10

3

4

- 5 Table 3. Elastic properties of the manufactured panels: median values and range (in parenthesis). Density values for the edgeways free vibration
- 6 bending are the same as the face down bending in the same direction.

Resin base	Cypress content (% wt.)	$E_x$ (GPa)		$E_y$ (GPa)			$G_{xy}$ (GPa)		$C_{zz}$ (GPa)		
		Face down bending		Face down bending			Edgeways free vibration		Density	Ultrasound	
		Density (kg m <sup>-3</sup> )	Static	Free vibration (~500 Hz)	Density (kg m <sup>-3</sup> )	static	Free vibration (~500 Hz)	Bending (~1.5 kHz)		(kg m <sup>-3</sup> )	(100 kHz)
								x sample	y sample		
Tannin	100	668 (35)	10.9 (0.3)	9.6 (2.7)	643 (23)	4 (0.1)	4.1 (0.6)	1.35 (0.4)	1.8 (1.9)	649 (40)	0.65 (0.25)
	75	658 (10)	8 (2.2)	7.7 (1)	667 (32)	4.9 (4)	5.1 (1.5)	1.3 (1.4)	0.9 (0.2)	705 (26)	0.61 (0.19)
	50	664 (15)	13.5 (1.4)	11.9 (3.1)	657 (15)	5.1 (1)	4.7 (1.8)	1.1 (0.7)	1 (0.5)	661 (61)	0.55 (0.18)
	0	650 (28)	5.4 (2.3)	7.8 (1.6)	667 (53)	3 (0.3)	3.3 (0.5)	0.7 (1.2)	2.1 (4.4)	690 (58)	0.36 (0.08)
Lignin	100	636 (27)	10 (1.9)	9.5 (0.6)	661 (68)	4.5 (1.5)	4.4 (1.2)	1.5 (1)	1.3 (1.4)	654 (153)	0.85 (0.38)
	75	673 (90)	12.9 (2.4)	11.2 (2.7)	628 (41)	4.9 (0.2)	4.9 (0.7)	1.6 (1)	1.3 (0.7)	636 (150)	0.67 (0.25)
	50	675 (37)	10.7 (2.3)	11.1 (0.8)	643 (46)	4.4 (4.4)	4 (0.7)	1.4 (0.4)	2.1 (1)	647 (174)	0.57 (0.39)
	0	664 (80)	12.1 (1)	11.3 (0.9)	652 (29)	3.4 (4)	5.9 (2.2)	1.1 (0.8)	1.1 (0.4)	643 (142)	0.52 (0.28)

7 **Figures' legend**

8

9 Figure 1. Cutting plan for specimens for measurements on the raw material.

10 Figure 2. Face view of a manufactured OSB (50% cypress-50% pine with the lignin based resin)  
11 and cutting plan

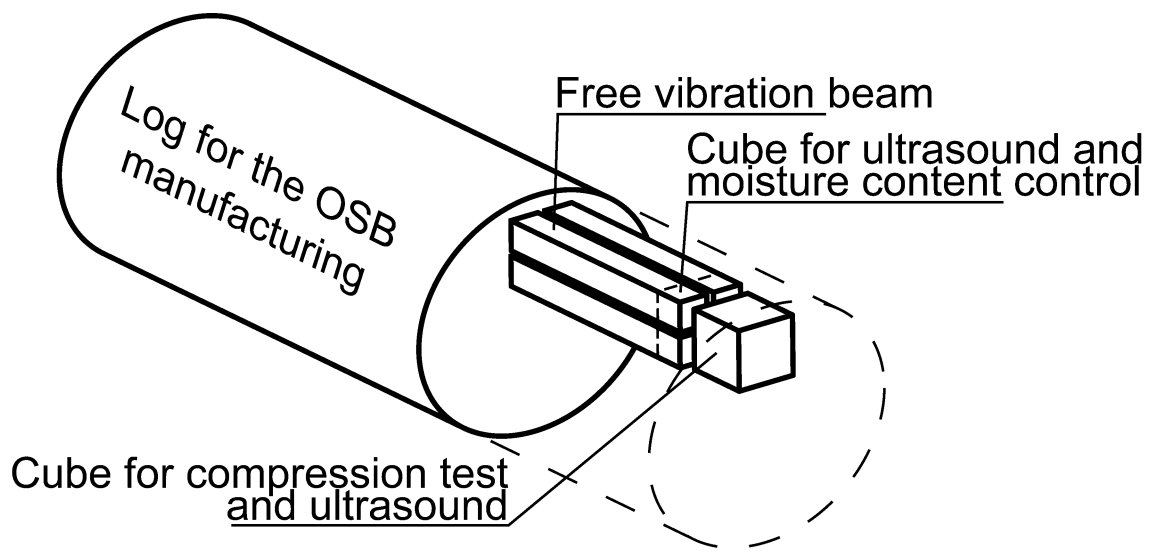
12 Figure 3. Characteristic measured density profile, DP, in thickness and layer-wise average for  
13 modelling purpose.

14 Figure 4. Strand orientations measured on the surfaces of three produced panels and normal  
15 distribution adjustment to the data ( $\mu = 0.4^\circ$ ,  $\sigma = 4.9^\circ$ ).

16 Figure 5. Comparison of experimental values from bending free vibration tests and corresponding  
17 model predictions.

18 Figure 6. Effect of strand orientation on the elastic bending constants.

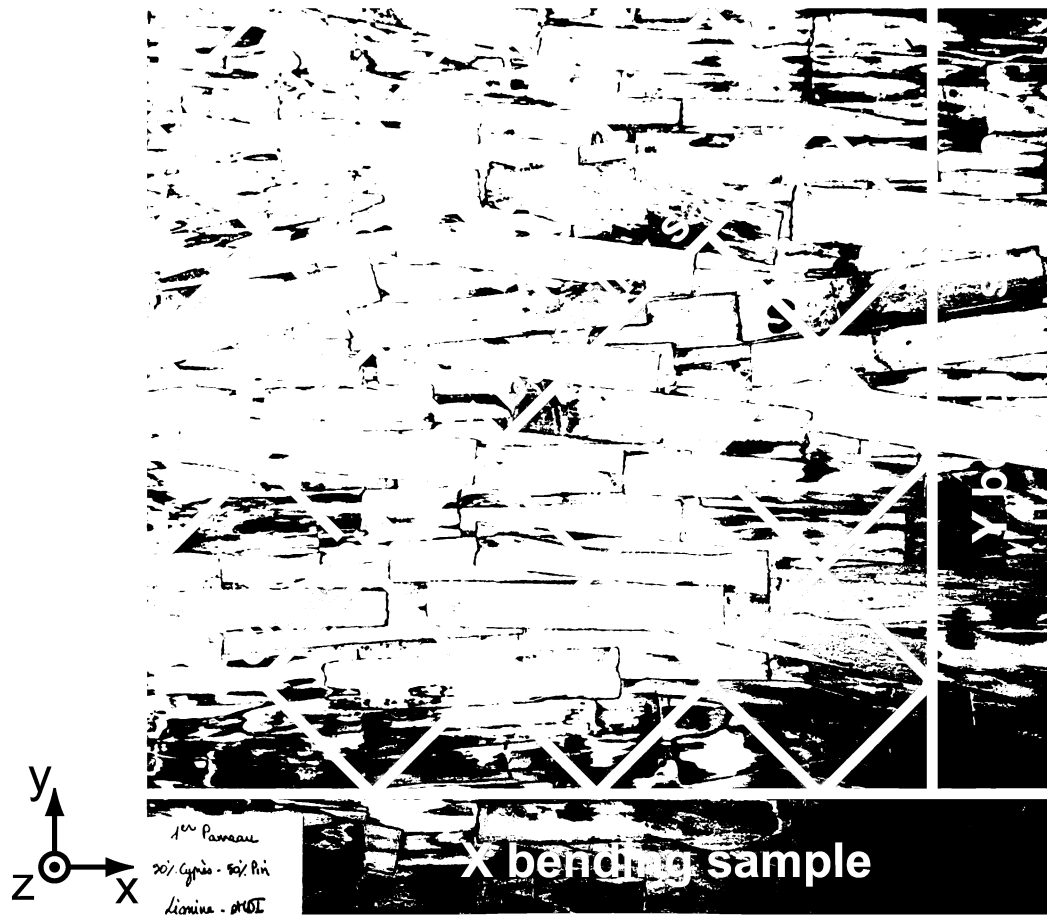
19



20

21 Figure 1. Cutting plan for specimens for measurements on the raw material.

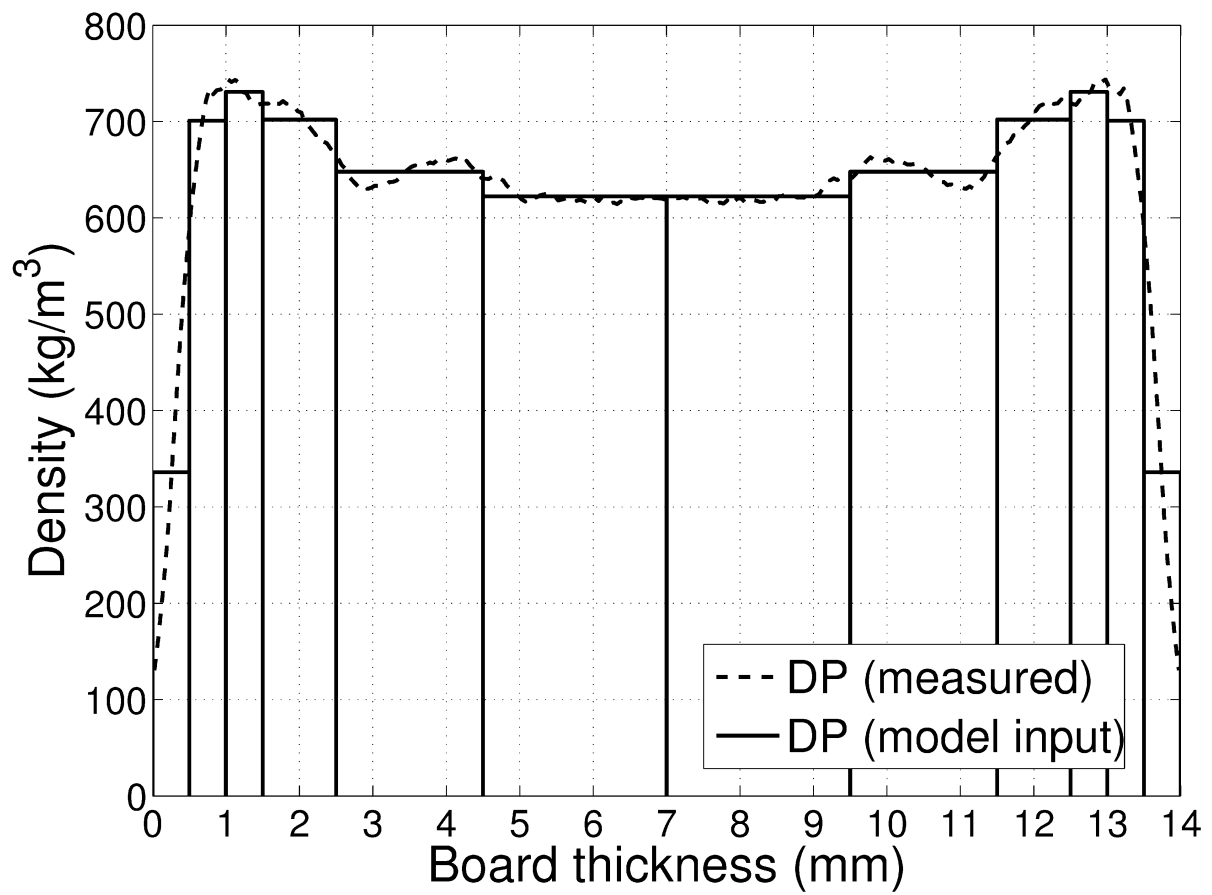
22



23

24 Figure 2. Face view of a manufactured OSB (50% cypress-50% pine with the lignin based resin)  
 25 and cutting plan.

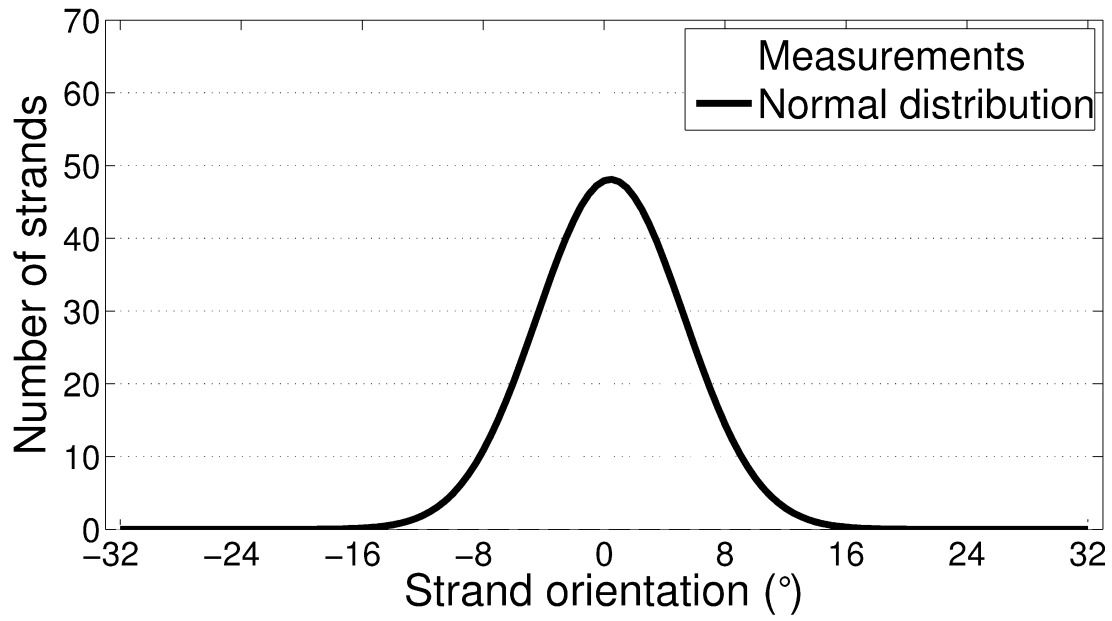
26



27

28 Figure 3. Characteristic measured density profile, DP, in thickness and layer-wise average for  
 29 modelling purpose.

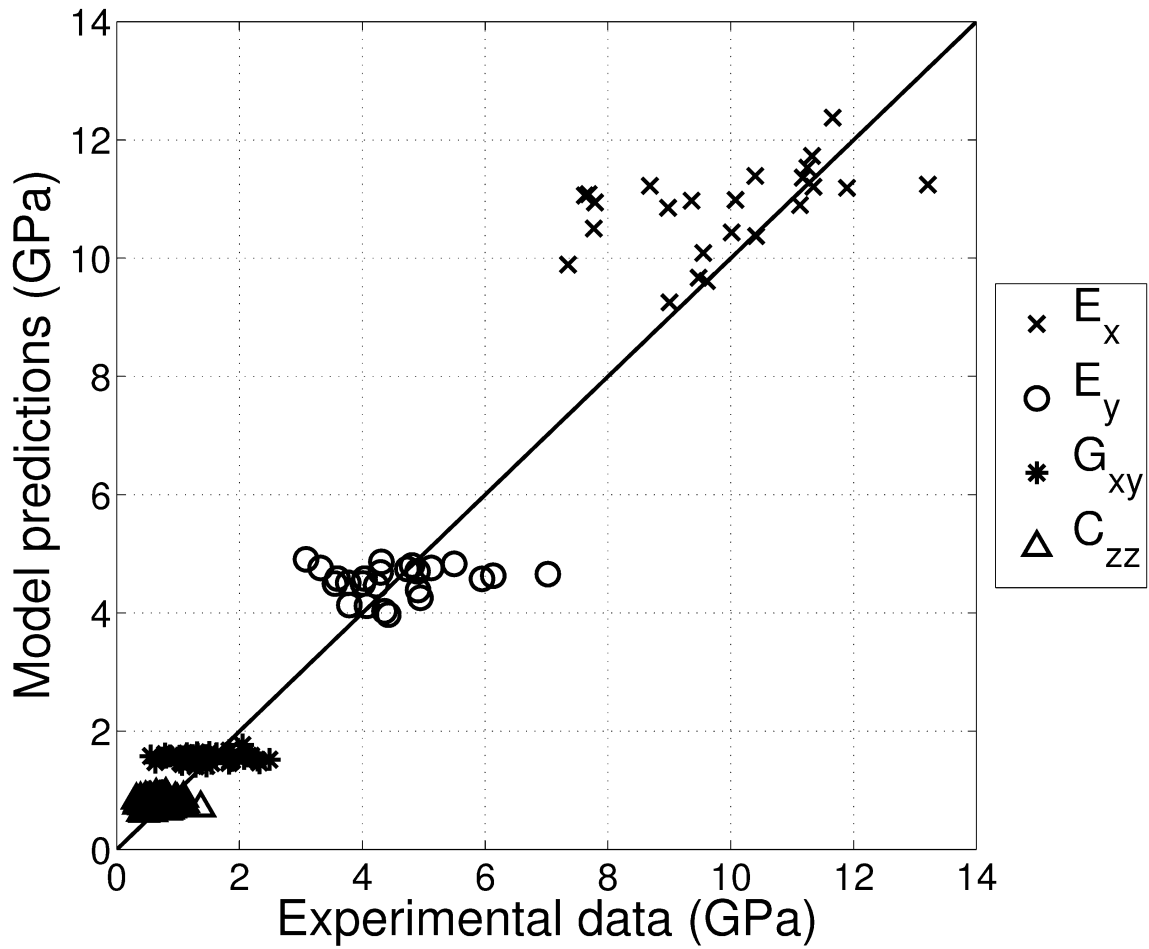
30



31

32 Figure 4. Strand orientations measured on the surfaces of three produced panels and normal  
33 distribution adjustment to the data ( $\mu = 0.4^\circ$ ,  $\sigma = 4.9^\circ$ ).

34

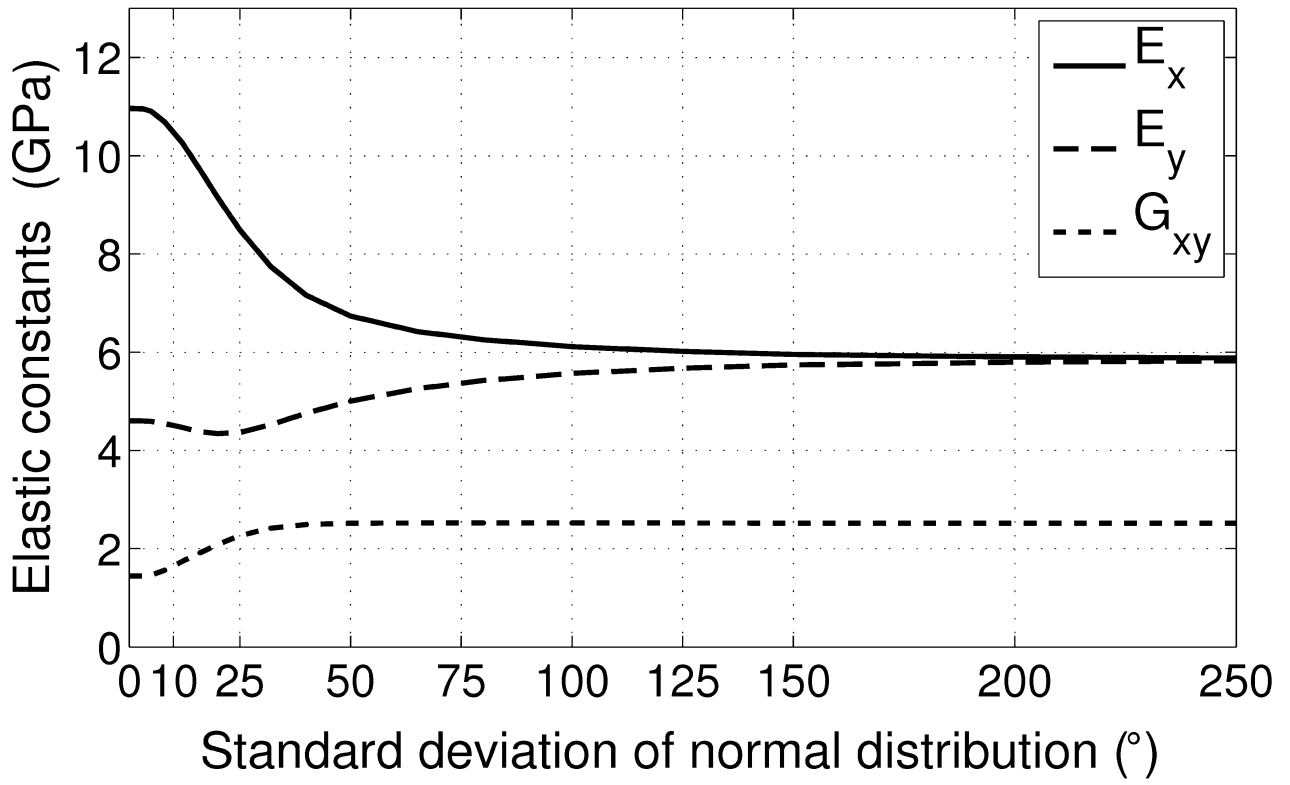


35

36 Figure 5. Comparison of experimental values from bending free vibration tests and corresponding  
 37 model predictions.

38





39

40 Figure 6. Effect of strand orientation on the elastic bending constants.